Evidence for Holocene environmental changes in the northern Fertile Crescent provided by pedogenic carbonate coatings

Konstantin Pustovoytov [a,*], Klaus Schmidt [b], Heinrich Taubald [c]

[a] *Institut für Bodenkunde und Standortlehre, Universität Hohenheim, Emil-Woll-Str. 27, 70599, Stuttgart, Germany*
[b] *Deutsches Archäologisches Institut, Podbielskiallee 69-71, 14195 Berlin, Germany*
[c] *Institut für Geowissenschaften, Universität Tübingen, Wilhelmstr. 56, 72074 Tübingen, Germany*

Abstract

Holocene environmental changes in the northern Fertile Crescent remain poorly understood because of the scarcity of local proxy records in the region. In this study we investigated pedogenic (soil-formed) carbonate coatings on stones at the Pre-Pottery Neolithic site Göbekli Tepe as an indicator of local early-mid Holocene environmental changes. The ^{14}C ages and stable isotopic composition of carbon and oxygen in thin (0.2–0.3 mm thick) pedogenic carbonate lamina indicate two main periods of coating formation: the early-Holocene (ca. 10000–6000 cal yr BP) and the mid-Holocene (ca. 6000–4000 cal yr BP). During the first period, there was an inverse relationship between δ^{13}C and δ^{18}O curves: a decrease in δ^{13}C values coincide with an increase in δ^{18}O values. For this period a trend towards higher temperatures is suggested. In the mid-Holocene, the mean rate of coating growth was 2–3 times higher than in the early Holocene. Both δ^{13}C and δ^{18}O reached their maximum values during this time and the direction of changes of the δ^{13}C and δ^{18}O curves became similar. The combination of data suggests that this period was the most humid in the Holocene and on average warmer than the early Holocene. At ca. 4000 cal yr BP secondary accumulation of carbonate ceased, presumably reflecting a shift to a more arid climate.
© 2007 University of Washington. All rights reserved.

Keywords: Pedogenic carbonate; ^{14}C dating; Stable carbon and oxygen isotopes; Holocene; Pre-Pottery Neolithic; Fertile Crescent

Introduction

As a region where the earliest farming economies in the world are suggested to have evolved, the so-called "Fertile Crescent" in the Near East has long been a focus of broad research interest (Childe, 1952; Braidwood and Howe, 1960; Van Zeist and Bottema, 1991; Goldberg, 1994; Zohary and Hopf, 2000; Robinson et al., 2006 and references therein). Over the last two decades, several lines of paleoenvironmental evidence for the eastern Mediterranean and the Near East have become available, which involve continuous, high-resolution proxy records: palynological and geochemical data from lacustrine (Bottema, 1995; Roberts et al., 1999, 2001; Yasuda et al., 2000; Snyder et al., 2001; Stevens et al., 2001; Wick et al., 2003) and marine (Rossignol-Strick, 1999) deposits, and stable isotope composition of speleothems (Bar-Matthews et al., 1997;

Bar-Matthews and Kaufman, 1998; Frumkin et al., 1999). Despite these studies, however, there is a deficit of paleoclimatic information for some regions of the Fertile Crescent, in particular for its northern part, Upper Mesopotamia. The main reason for this data shortage is probably the scarcity of sediments potentially suitable for pollen analysis, such as lake deposits. Interestingly, it is precisely this region that provided carpological (Nesbitt, 2002 and references therein) and genetic (Heun et al., 1997) evidence of the earliest cereal domestication, which emphasizes its importance for our understanding of agricultural origins.

In this study we investigate pedogenic carbonate laminations on stones at the Pre-Pottery Neolithic site Göbekli Tepe in Upper Mesopotamia (southeastern Turkey) to obtain indications of environmental change in the Holocene. Accumulation of pedogenic carbonate on stones is a relatively slow process, mostly resulting in formation of a succession of laminae that may differ in their properties (colour, transparency, admixtures, etc.), reflecting changing conditions of coating growth over

time (Courty et al., 1994; Pustovoytov, 2002). Isotopic composition of carbon and oxygen in pedogenic carbonate is sensitive to the environment of soil formation (Cerling, 1984; Amundson et al., 1989; Quade et al., 1989). This feature provides a basis for a wide range of paleoclimatic reconstructions. Specifically, pedogenic carbonate rinds on gravels have been used as indicators of late-Quaternary paleoecological conditions in some areas of North America (Wang et al., 1996; Monger et al., 1998; Buck and Monger, 1999; Deutz et al., 2001).

The aims of this study were as follows: (1) to establish a ^{14}C chronological framework for the formation of pedogenic carbonate coatings on stones of the site by dating their individual thin laminae; (2) to provide a record of δ^{13}C and δ^{18}O values of the carbonate fraction in a continuous sequence of coating laminae; and (3) to interpret relative shifts in the isotopic composition of pedogenic carbonate over time in terms of environmental change and to compare the coating archive with other proxy records available for the region. The approach in the present work is novel in two respects. First, to our knowledge it represents the first attempt to derive a continuous proxy record from successions of laminae of pedogenic carbonate on stones. We could not find published examples of systematic, high-resolution sampling of pedogenic carbonate in thin layers followed by isotopic measurements, although some authors reported results of examining the inner and the outer microlayer (hereafter the term "microlayer" is used as a synonym for "laminae") of a coating separately (Amundson et al., 1989; Wang et al., 1996). Second, we had reliable independent chronological control to compare with radiocarbon ages of individual microlayers because we studied secondary carbonate on stones from intact architectural structures of an archaeological site of known age. In contrast, absolute-age estimations based on the chronology of relief forms (river terraces, dunes, etc.) used as references in previous works involving ^{14}C dating of pedogenic carbonate coatings have relatively low resolution (e.g., Amundson et al., 1994 and references therein; Wang et al., 1996; Monger et al., 1998; Buck and Monger, 1999; Deutz et al., 2001).

Site description

Göbekli Tepe (37°13′N, 38°55′E) is located at the south margin of the Taurus Mountains, northeast of Şanliurfa at ca. 800 m a.s.l. (Fig. 1), on the top of one of the Eocene limestone ridges (Pamir and Erentöz, 1974) highly dissected by erosion. The climate of Şanliurfa is typical Mediterranean: hot and dry summers (mean July temperature and precipitation are 30.8 °C and 0.3 mm, respectively) with mild and relatively humid winters (mean January temperature 5.9 °C, mean January precipitation 93.1 mm) (Alex, 1985). The vegetation around the site is almost completely a grass steppe dominated by *Hordeum spontaneum*, *Avena* sp., *Bromus* sp., *Stipa* sp. and *Aegilops* sp. (Neef, 2003). In the soil cover of the region around Şanliurfa, Calcic Xerosols associated with Chromic Luvisols prevail (Straub, 1988) (after the WRB nomenclature (1998) these are Aridic Calcisols and Lithic Leptosols, respectively).
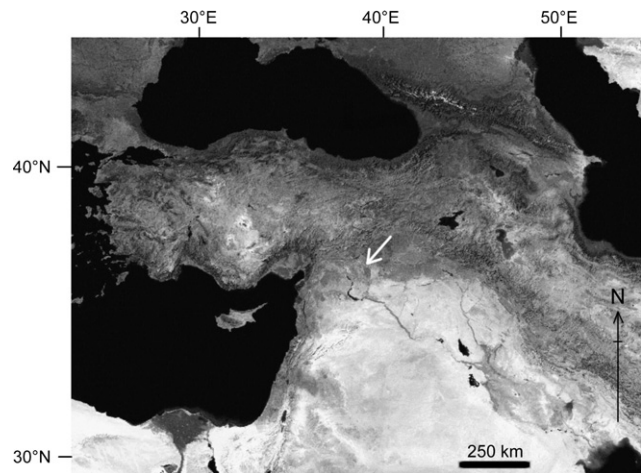

Figure 1. Map showing the location of Göbekli Tepe (arrow).

Archaeologically, Göbekli Tepe is a Pre-Pottery Neolithic (PPN) site. Within the PPN period there are two main phases, PPNA and PPNB, that both have been identified at Göbekli Tepe. The numerical age ranges for PPNA and PPNB are considered here to be approximately 11,750–10,750 and 10,750–8350 cal yr BP, respectively (Aurenche et al., 2001). Further differentiation among PPNB periods is as follows: the Early PPNB (EPPNB) 10,750–10,250 cal yr BP, the Middle PPNB (MPPNB) 10,350–9450 cal yr BP and the Late PPNB (LPPNB) 9550–8350 cal yr BP (Aurenche et al., 2001).

The site consists of several artificial mounds of which the highest one is about 15 m high. A total area occupied by the mounds of Göbekli Tepe is ca. 9 ha. The most characteristic feature of the site is represented by architectural complexes, which are oval and rectangular stone buildings with megalithic T-shaped limestone pillars (Schmidt, 2001, 2002, 2003; Peters and Schmidt, 2004). No indication of a sedentary occupation has been found hitherto at Göbekli Tepe; the site obviously served exclusively as a ritual building complex (Schmidt, 2003). Immediately before the abandonment, all architectural constructions were intentionally covered by fill (stones with fine earth), which gave rise to soil development after a relatively short time-span needed for stabilization of the site surface. There were presumably at least two phases of such burials—during the PPNA/EPPNB and during the MPPNB periods (Schmidt, 2003). No archaeological evidence of a systematic occupation of the site after PPNB has been found (Schmidt, 2001, 2003). However, there is a post-PPNB artificial disturbance of problematic origin in the fill in form of a pit seen at the western wall of trench L9-87 and a pottery shard not older than Roman in age in the lower part of a 1- to 2-m eluvial deposit at the toe-slope (Schmidt, 2003).

Materials and methods

General features of soils and pedosediments at Göbekli Tepe have already been given in a previous report (Pustovoytov, 2006); therefore, we restrict our consideration here only to the Bk horizon (soil horizon nomenclature according to Birkeland, 1999, and the Guidelines for Soil Profile Description, 1990). The

Bk horizon at the site represents a continuous zone with distinct indications of secondary carbonate accumulation, which runs subparallel to the site surface. The visible part of Bk horizon exposed by excavation is 1–1.5 m in thickness. Pedogenic carbonate is present in form of coatings on the undersides of large clasts in the fill (stones, large fragments of bones, lithic tools) and wall stones in architectural structures and on the lower surfaces of convex elements in relief representations at T-shaped pillars. A uniform orientation of secondary carbonate accumulations on all clasts within the Bk horizon provides a clear indication that the carbonate accumulation took place in situ, after the abandonment of the site, and is inherently pedogenic. In the upper half of the Bk horizon there is a ca. 20- to 30-cm-thick zone of maximum secondary carbonate accumulation where the coatings are at their thickest (on the order of 5 mm).

Fragments of stones with secondary carbonate accumulations were collected in the field after examination of the vertical distribution of coatings. Coating samples studied in this work were taken mostly from the upper half of the Bk horizon, where their thickness was greatest. Four coating samples originated from PPNA-EPPNB contexts, two from MPPNB, one from a post-MPPNB and one from a post-LPPNB context (Fig. 3). There was also one sample of a pre-PPNA coating, which was located at the same depth as the coating L9-80[1] and less than 1 m from it. In contrast to all other secondary carbonate laminations, this coating covered the upper surface of a stone in the wall in trench L9-80 (Fig. 5), clearly indicating its formation before the construction of the wall. It differed from the rest of the coatings by its reddish pigmentation. It thus can serve as an indicator of diagenetic ^{14}C contamination of the coating L9-80.

In the laboratory, coatings together with stone fragments they covered were first interposed in gypsum to further stabilize samples prior to sawing. Samples were then cut with a diamond saw in slices ca. 3–7 mm thick to obtain series of cross sections of coatings. Five such slices were used for preparing thin sections for micromorphological observations. The coatings' micromorphology was studied with a petrographic microscope, following the recommendations of Bullock et al. (1985) and Courty et al. (1989). Scanning electron microscopy was investigated with Zeiss DSM 940 (coating Au (80%) and Pd (20%), working voltage 5000 V).

Material for isotopic measurements and ^{14}C dating was bored out with a goldsmith drill from the cross sections of coatings on stones, under a stereoscopic microscope. In boring, special effort was made to follow the extension of individual laminae of pedogenic carbonate with the drill and, in case of the innermost (oldest) laminae, to avoid contact of the drill with the primary limestone. The thicknesses of the sampled laminae were 0.2–0.3 mm. Two sequences of microlayers were obtained for coating samples L9-66 and L9-80 from ca. 100 and 85 cm below the soil surface, respectively. Coating L9-80 provided a series of 16 samples and coating L9-66 yielded 32 samples from an exceptionally thick fragment, although some of the latter

samples contained too little material and produced no measurement result (Fig. 5).

Samples of primary limestone were taken from fresh outcrops exposed by road works in the immediate vicinity of the site. Soil samples for estimations of $\delta^{13}C$ of organic carbon were collected from 5 profiles (Fig. 3i).

Stable isotope analysis was performed at the Institute of Geosciences of the University of Tubingen, Germany, using a Finnigan MAT 252 gas source mass spectrometer combined with a ThermoFinnigan GasBench II/CTC Combi-Pal auto-sampler (Spötl and Vennemann, 2003). Prior to measurements for stable carbon isotope composition, samples were reacted with 3% HCl to remove carbonate.

For both successions of laminae L9-66 and L9-80, the carbonate fraction of the innermost (oldest), the middle and the outermost (youngest) microlayers was dated by [14]C. Additionally, the carbonate fractions of the oldest microlayers in an additional 6 coatings were dated by [14]C. The ^{14}C measurements (AMS) on pedogenic carbonate were performed at the Leibniz-Laboratory at the University of Kiel and at the Ångström Laboratory at the University of Uppsala, Sweden. All ^{14}C results were normalized to $\delta^{13}C = -25‰$ and calibrated with the OxCal v3.5 program (Ramsey, 2001).

Results and discussion

Morphology of pedogenic carbonate coatings

The pedogenic carbonate coatings are composed of calcite associated with groundmass (Figs. 2b–e). Most of the calcite consists of sparitic and microsparitic crystals that are parallel or randomly arranged (Figs. 2d, e, g, h) and show a distinct rhombohedral shape without obvious signs of dissolution (Fig. 2h). Much of the groundmass is presumably impregnated by micritic secondary calcite, which is evident from the dominant pale grey colour of peds in plane polarized light and their scattered high interference colours in crossed polarized light. Small bone fragments less than 0.5 mm in length are sporadically incorporated into the coatings (Figs. 2b, d). Although on the basis of (sub)micromorphology alone it cannot be excluded that secondary carbonate laminations at Göbekli Tepe may contain some admixture of primary carbonate in the micritic fraction, no explicit forms of limestone fragments were found.

An important feature of secondary carbonate laminations is dark-coloured, elongated to isometric particles on the order of 0.05–0.1 mm in length (Figs. 2a, f, i–l), which can be found occasionally within the inner zone of coatings and constitute about 1/5–1/3 of the total coating thickness. These dark particles are characterized by distinct biogenic structures (Figs. 2i–l) and most probably represent fragments of plant tissues (presumably charred to some extent), occluded into precipitating carbonate at an early stage of formation.

[14]C age of pedogenic carbonate laminae

Pedogenic carbonate forms in isotopic equilibrium with soil CO_2 (Cerling, 1984) and therefore is expected to be

---

[1] Hereafter coatings L9-66 and L9-80 are called according to the trench nomenclature in the excavation map where the samples were collected (Fig. 3).
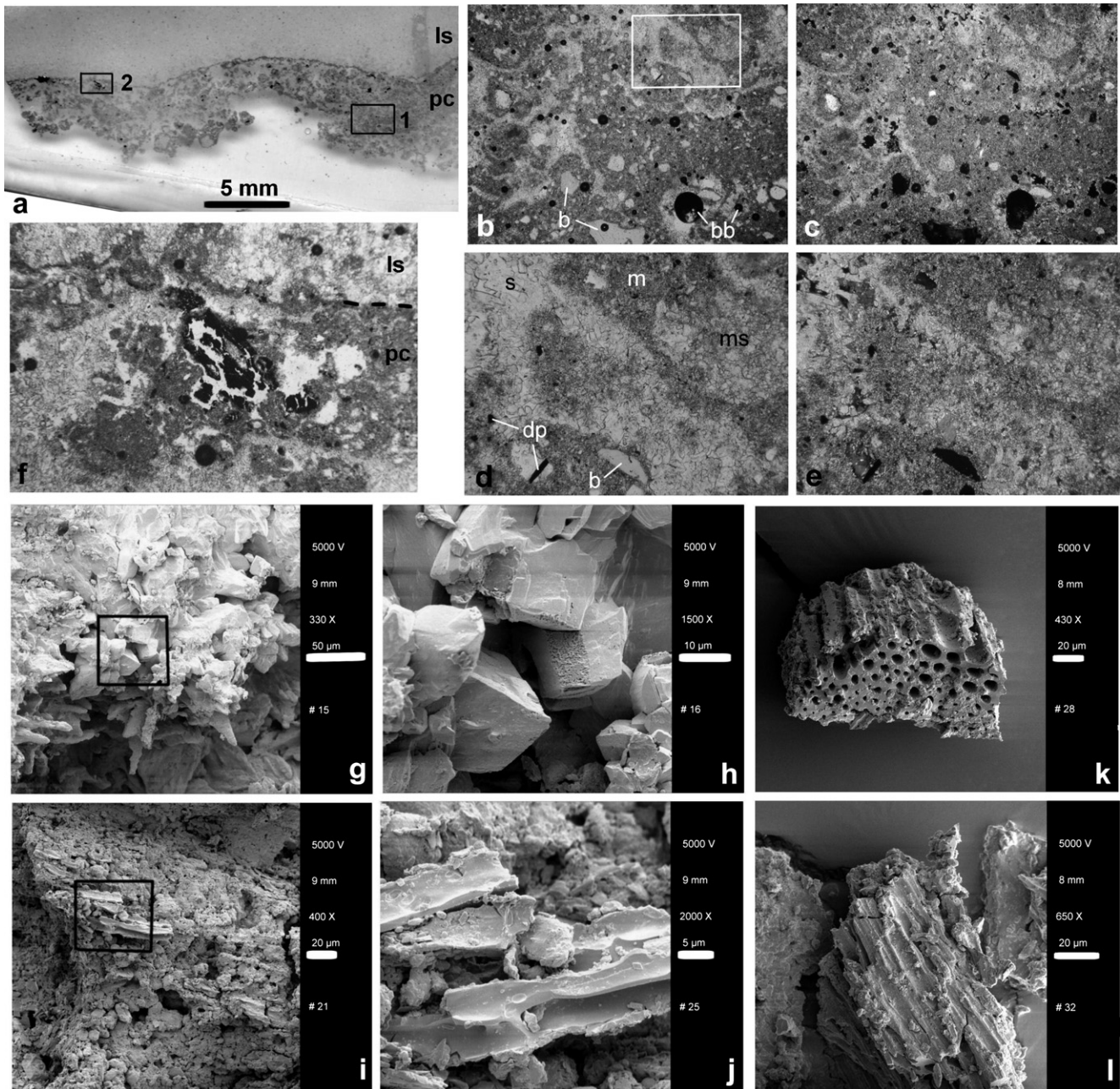
Figure 2. Micromorphology and SEM of pedogenic carbonate accumulations: (a) Fragment of the thin section of a pedogenic carbonate coating from trench L9-66, 105 cm below the soil surface at low magnification; ls—primary limestone, pc—pedogenic carbonate coating. (b) Fragment marked by frame 1 in panel a, parallel polarizers (PPL); several lamination layers are distinctly seen on the left. b—bone fragment, bb—bubbles (from thin-section preparation). (c) Same as in panel b but with crossed polarizers (XPL). (d) Fragment marked in panel b by frame, PPL: s—a buildup of sparitic calcite crystals randomly arranged but in places with a parallel motive, ms—microsparitic calcite, m—micritic calcite most probably associated with dispersed silty-clayey groundmass, dp—small dark-coloured particles, b—bone fragment. (e) Same as in panel d but XPL. (f) Fragment marked by frame 2 in panel a; PPL: a relatively large dark-coloured particle in the oldest generation of pedogenic carbonate laminations at the limestone-coating interface is distinctly seen in centre; ls—primary limestone, pc—pedogenic carbonate coating, dotted line—limestone-pedogenic carbonate boundary. (g–l) SEM images: (g) randomly and radially oriented microsparitic and sparitic calcite crystals; scale bar 50 µm. (h) Fragment marked in panel g. Microsparitic calcite crystals; scale bar 10 µm. (i) Dark particle (left-hand of the image centre) in a matrix aggregate; scale bar 20 µm. (j) Fragment marked in panel i; structures resembling vessels of plant tissues are seen; scale bar 5 µm. (k and l) Two relatively large dark-coloured particles separated from the coating; note the obvious tissue-vessel structure; Scale bars 20 µm.

suitable substrate for ^{14}C dating (Amundson et al., 1994; Wang et al., 1996; Monger et al., 1998; Buck and Monger, 1999; Deutz et al., 2001). However, several complicating factors represent potential limitations of the applicability of ^{14}C method to pedogenic carbonate. One is that radio-metrically "dead" carbon can be introduced into crystallizing secondary carbonate, either mechanically, as admixtures of older calcareous fragments (Amundson et al., 1989; Monger et al., 1998; Khokhlova et al., 2004), or chemically, through utilization of carbon of old organic matter and its subsequent

respiration in the form of CO_2 by microorganisms (Wang et al., 1994). A second factor is diagenetic recrystallization of carbonate in soil in the course of pedogenesis (Pendall et al., 1994; Pustovoytov and Leisten, 2002; Khokhlova et al., 2004). Furthermore, if the whole material of pedogenic carbonate is dated, interpretation of radiocarbon age can be difficult because of varying rates of carbonate accumulation during the time of soil formation (Amundson et al., 1994; Wang et al., 1996). At Göbekli Tepe, three regularities suggest that secondary carbonate laminations did form in carbon isotopic equilibrium with soil CO_2 without substantial contribution of primary limestone carbonate or diagenetic recrystallization of pedogenic carbonate (Table 1, Figs. 3 and 4). First, all dates for the innermost lamina on stone constructions are generally younger than the estimated age-constraints for their archaeological contexts, and they uniformly decrease with decreasing context age. Second, except for sample L9-76, there is a high degree of consistency between the ^{14}C ages obtained for the oldest coating laminae from the same PPN contexts. Such a conformity is unlikely to result from a coincidental equality of concentrations of carbon from a variety of sources (such as soil carbon dioxide and limestone) and can be best explained in terms of formation of secondary carbonate in isotopic equilibrium with soil CO_2 at an early stage of pedogenesis. Because of the limited number of dates, currently it appears difficult to explain the variance in the measured ages of the oldest microlayers of pedogenic carbonate, such as the comparatively young ^{14}C age in sample L9-76. We hypothesize that it may reflect differences in the time when carbonate accumulation began, small variations in the thickness of bored-out microlayers, discontinuities of individual laminae of pedogenic carbonate or differences in their accumulation

rates. An extended data set would be needed to answer this question.

The third regularity is that two sequences, each including three microlayers, demonstrate a distinct decrease in radiocarbon ages from the inner to the outer secondary carbonate laminations. There is also a reasonably good agreement in the ages between the two middle coating microlayers and the two outer (youngest) laminae.

Although we cannot exclude diagenetic alteration of pedogenic carbonate that could lead to ^{14}C contamination, a relatively old age—10,210 ^{14}C yr BP—of the youngest microlayer of the pre-PPNA coating suggests that such a process is unlikely to have substantially affected the radiocarbon ages of pedogenic carbonate accumulations. Furthermore, diagenetic radiocarbon contamination would be hard to reconcile with the close agreement between the two ^{14}C ages for the youngest laminae of coatings L9-66 and L9-80 from different trenches of the site. For the innermost microlayers , the probability of diagenetic alteration is even lower than for the outermost ones because of the protective role of younger laminae. It is thus not surprising that all dates for the innermost lamina are concordant and that their ^{14}C content is relatively low and typical for early Holocene carbon-containing materials. A consideration of the set of ^{14}C dates for secondary carbonate coatings therefore leads to the conclusion that the measured radiocarbon ages approximate the time of formation of individual microlayers of pedogenic carbonate.

Two successions of microlayers in coatings L9-66 and L9-80 suggest that the accumulation of pedogenic carbonate occurred mostly in the early Holocene and ceased late in the mid-Holocene. The radiocarbon ages of the innermost carbonate microlayers strongly indicate an almost simulta-

Table 1
Radiocarbon ages of microlayers of pedogenic carbonate coatings

Trench	Archaeological context	Microlayer	Laboratory number	Age (^{14}C yr BP)	Calibrated age (cal yr BP) (2σ-range)	Probability, %	Mean weighted*
L9-66	PPNA-EPPNB	Oldest	Ua-19562	8960±85	10,250–9750	95.4	10,000
L9-66	PPNA-EPPNB	Middle	KIA-23389	5450±35	6310–6170	95.4	6240
L9-66	PPNA-EPPNB	Youngest	KIA-23388	4045±35	4790–4760	3.6	4525
					4620–4410	91.8	
L9-80	MPPNB	Oldest	KIA-26168	8625±45	9730–9520	95.4	9625
L9-80	MPPNB	Middle	KIA-26274	4640±30	5470–5350	76.8	5234
					5340–5300	18.6	
L9-80	MPPNB	Youngest	KIA-26273	3735±30	4230–4200	2.4	4074
					4160–3980	93.0	
L9-80	Pre-PPNA	Youngest	KIA-28405	10210±50	12,350–11,600	95.4	–
L9-65	PPNA-EPPNB	Oldest	KIA-26021	9020±30	10,240–10,150	95.4	–
L9-76	PPNA-EPPNB	Oldest	Ua-19561	8430±80	9550–9260	93.9	–
					9170–9150	1.5	
L9-79	PPNA-EPPNB	Oldest	KIA-25373	8895±55	10,210–9770	95.4	–
L10-71	MPPNB	Oldest	KIA-26169	8440±40	9540–9400	90.5	–
					9350–9320	4.9	
L9-56	Post-MPPNB	Oldest	KIA-28033	7180±40	8120–8080	9.0	–
					8050–7930	80.2	
					7900–7870	6.1	
L9-87	Post-LPPNB	Oldest	Ua-21416	6405±70	7440–7180	95.4	–

*Calculated for ^{14}C ages of microlayers from L9-66 and L9-80 to ease correlation (Fig. 8).
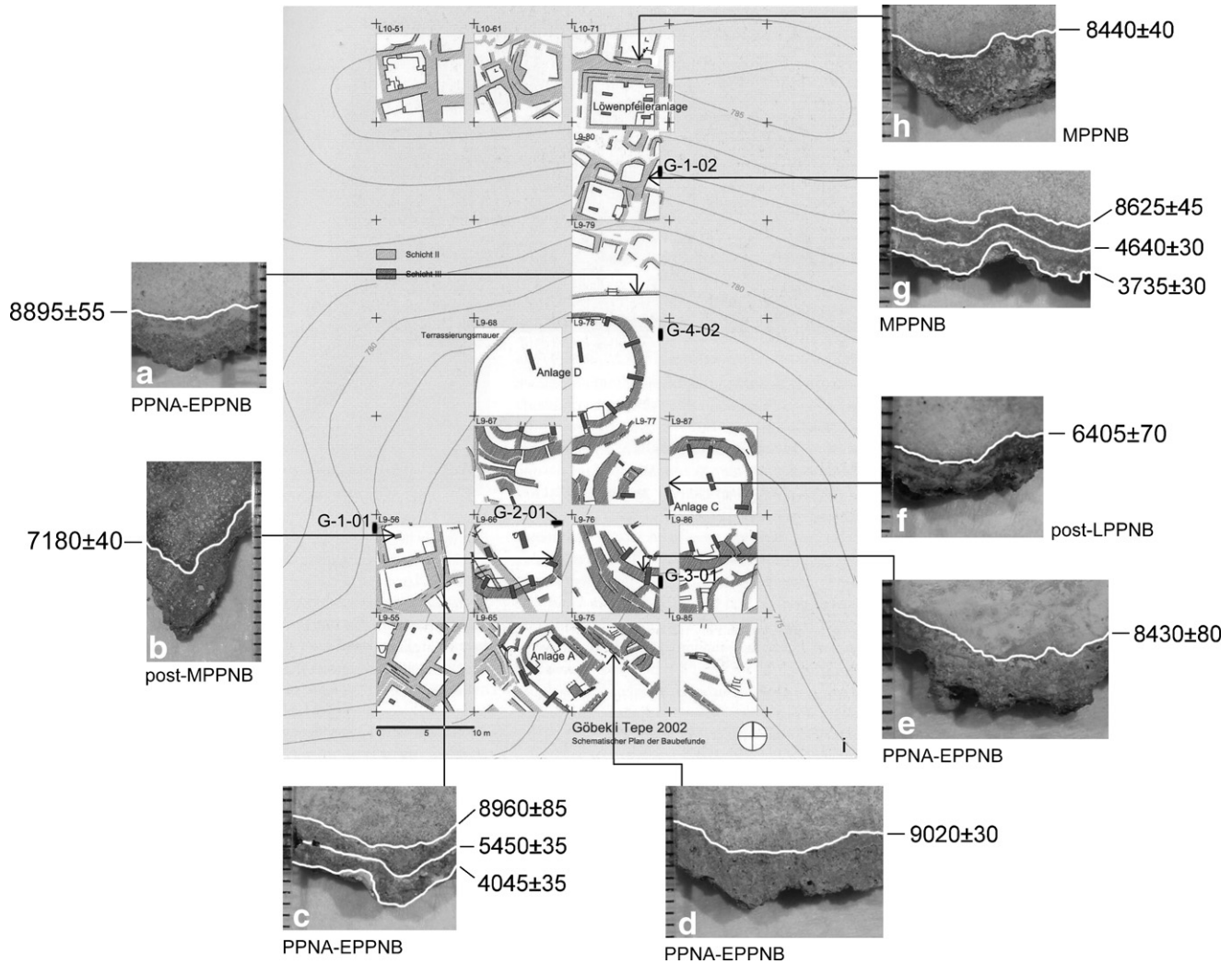
Figure 3. Pedogenic carbonate coatings on stones from archaeological contexts at Göbekli Tepe and their ^{14}C ages. Arrows connect the photographs of cross sections of pedogenic carbonate coatings (a–h) with their sampling locations on the map of the excavated area and relief of the mound (Kurapkat, 2004) (i). Isotypes are shown by dark grey lines on the light-grey field around the excavation trenches; the height is given in meters above the sea level. Black bars show the positions of profiles G-1-02, G-4-02, G-1-01, G-2-01 and G-3-01 tested for δ^{13}C of soil organic matter (Fig. 6). All cross sections show the coatings in their natural orientation, i.e. on the undersides of stones. Scale in coating photographs in mm. Note that most of the coatings are darker pigmented than the limestone (presumably through soil organic matter). White lines in the coating photographs indicate the microlayers sampled and dated with ^{14}C method. Radiocarbon ages are given uncalibrated in ^{14}C yr BP.
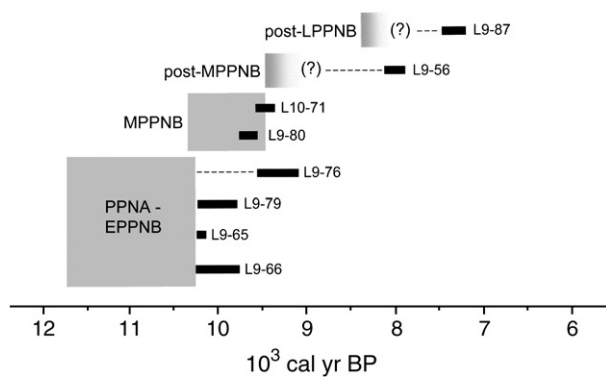

Figure 4. Comparison of the calibrated radiocarbon ages of the oldest laminae of pedogenic carbonate coatings with expected age ranges of archaeological contexts. 2σ intervals of radiocarbon ages on secondary carbonate presented as black bars. The chronology of PPN periods is given after Aurenche et al. (2001).

neous start of coating formation, which most probably corresponds to the beginning of soil formation on the surface of buried stone constructions. The ^{14}C ages imply that the coating thickening was non-linear in time: the second half of the coating thickness grew over the order of 1000–1500 yr with a mean rate of about 1.5–2 mm/ka (taking the coating thickness to be 5 mm), whereas the first one accumulated over a period of some 4000–5000 yr suggesting a mean growth rate of approximately 0.6–0.7 mm/ka. We assume that climatic changes in the early to mid-Holocene governed the coating growth. Higher rates of pedogenic carbonate formation during the mid-Holocene can be explained by a change to more humid climatic conditions, which could have caused an intensification of carbonate leaching from the upper parts of soil profiles and, as a consequence, an enhanced supply of bicarbonate solution to the Bk horizons.
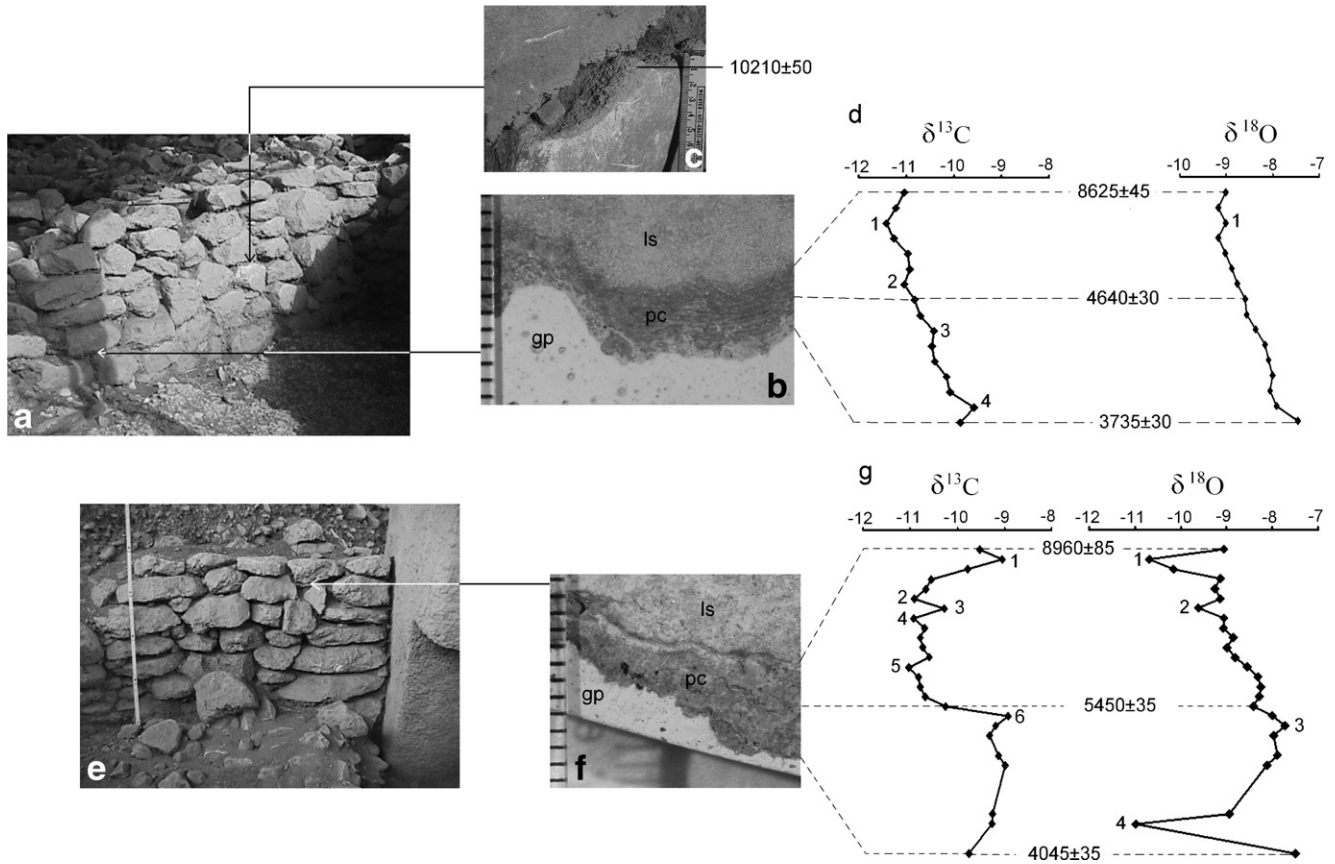
Figure 5. Stable isotopic composition of carbon and oxygen in two successions of pedogenic carbonate microlayers, L9-66 and L9-80, and their collection sites at Göbekli Tepe. (a) Stone wall in trench L9-80; arrows show the sampling locations of coating L9-80 and of the pre-PPNA coating. Note that prior to excavation, the soil surface was located some 30 cm above the uppermost stone row; scale length on top of wall 24 cm. (b) Cross section of a fragment of the coating L9-80: pc—pedogenic carbonate laminations, ls—primary limestone, gp—gypsum (used for stabilizing the sample prior to sawing); scale in mm. (c) A pre-PPNA secondary carbonate coating covering the upper side of a stone; the ^{14}C age is for the outer microlayer of the coating; scale in cm. (d) The δ^{13}C and δ^{18}O values (‰) of pedogenic carbonate microlayers in coating L9-80 with ^{14}C ages of the oldest, middle and youngest microlayers; numbers indicate peaks discussed in text. (e) Stone wall in trench L9-66; arrow indicates the sampling point of coating L9-66. Visible scale length 1 m. (f) As in panel b for coating L9-66. (g) As in panel d for coating L9-66. All ages are given as uncalibrated ^{14}C yr BP.

Analogously, the termination of accumulation of pedogenic carbonate is assumed to reflect an increased aridity of climate.

Figure 6. δ^{13}C values of soil organic matter in profiles shown in Figure 3i.

Stable isotope composition of carbon and oxygen in sequences of pedogenic carbonate microlayers

δ^{13}C values

The δ^{13}C values for pedogenic carbonate in two successions of pedogenic carbonate microlayers (Fig. 5) support the conclusion made above, based on the ^{14}C ages, that pedogenic carbonate forms in equilibrium with soil CO_2 in terms of carbon isotopes. The δ^{13}C is of the order of −10‰, which is distinctly more negative than that of the limestone and about 15‰ higher than the δ^{13}C values of soil organic matter (around −25‰) (Figs. 6 and 7). Such a difference between

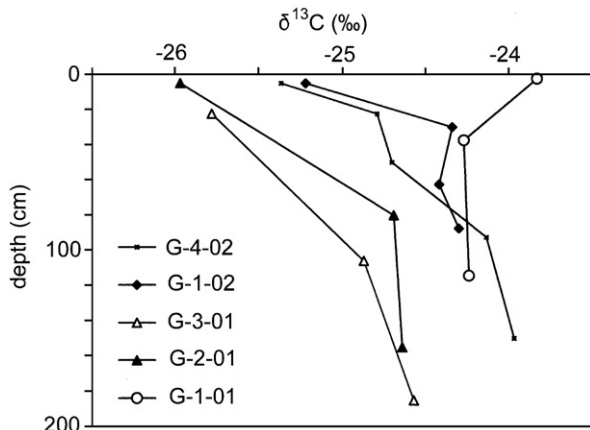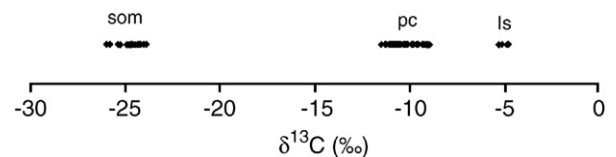Figure 7. Comparison of the stable carbon composition of pedogenic carbonate (pc) with that of soil organic matter (som) and primary limestone (ls).

$\delta^{13}C$ values of pedogenic carbonate and soil organic substances strongly indicates that the principal source of the inorganic carbon in secondary coatings is CO_2 respired by plant roots and soil microflora (Cerling, 1984; Cerling et al., 1989).

Both studied successions of pedogenic carbonate laminae display a general trend towards more positive $\delta^{13}C$ values from the first half of the Holocene to the mid-Holocene (Figs. 5 and 8). The similarity in tendencies between two coatings suggests that pedogenic carbonate at the site is most likely to have recorded paleoclimatic signals. A more detailed consideration reveals that every curve has several pronounced minima: 1 and 2 in curve L9-80 and 2, 4 and 5 in curve L9-66. There are also some distinct positive peaks in curve L9-66, which are 1, 6 and (less pronounced) 3. Positive peaks in curve L9-80 (3 and 4) are less pronounced; curve L9-66 has more abundant peaks than L9-80. At present it remains unclear whether this difference reflects local conditions of secondary carbonate formation, or is due to a more detailed sampling of the coating from trench L9-66.

Since the carbon isotopic composition of pedogenic carbonate at Göbekli Tepe is controlled by soil CO_2, several possibilities can explain positive shifts in $\delta^{13}C$ values of pedogenic carbonate laminations:

(1) Increase in C4 plant biomass (Nordt et al., 1996, and references therein; Sage, 2001, and references therein). The proportion of C4 plant biomass during the Holocene at Göbekli Tepe was presumably low, as exemplified by the $\delta^{13}C$ values of

soil organic matter (Ambrose and Sikes, 1991; Mora and Pratt, 2002) (Fig. 6). However, even if minor, an admixture of C4 plants might have caused an increase in $\delta^{13}C$ of pedogenic carbonate (characteristic carbon isotopic signatures in C3 and C4 plants (Cerling and Quade, 1993) suggest that a $\delta^{13}C$ increase of pedogenic carbonate of about 2‰ corresponds to a ca. 15% increase in the proportion of C4 biomass).

(2) Specific photosynthetic reactions of C3 vegetation. An increase in $\delta^{13}C$ values of tissues of C3 plants, for example, can be due to environmental conditions such as water stress (Williams and Ehleringer, 1996; Araus et al., 1997; Warren et al., 2001; Ferrio et al., 2003), deterioration of low temperatures (Körner et al., 1991) or a decrease in the canopy effect (Schleser and Jajasekera, 1985; Tieszen, 1991).

(3) Decrease in soil respiration rates. Lower soil respiration rates result in higher $\delta^{13}C$ values of soil CO_2 and pedogenic carbonate (Cerling, 1984, 1991).

(4) Decrease in the density of the vegetation cover. It is assumed that soil air can be enriched in CO_2 of atmospheric origin and thus increase $\delta^{13}C$ values of pedogenic carbonate if the density of vegetation over a soil is low (Wang et al., 1996; Monger et al., 1998).

Some of these explanatory options (3 and 4) do not reconcile the generally more positive composition of stable carbon isotopes in pedogenic carbonate at Göbekli Tepe in the mid-Holocene with the higher intensity of secondary carbonate accumulation during that period. Furthermore, it would be also difficult to attribute the higher $\delta^{13}C$ values of coating laminae to
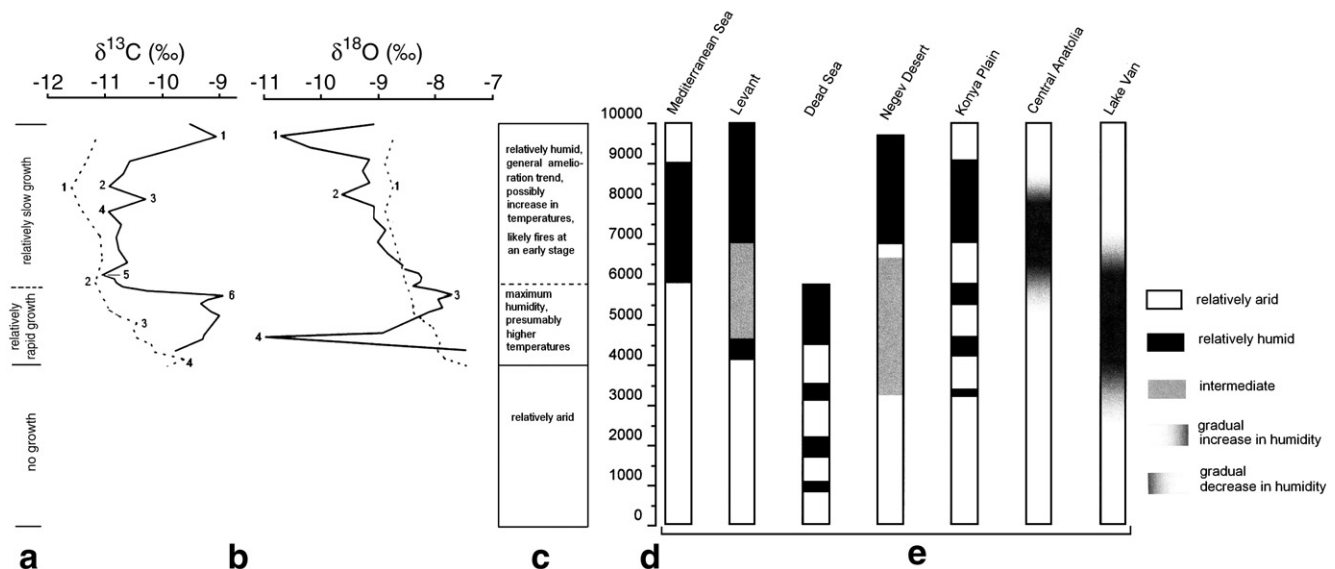

Figure 8. Comparison of the isotopic signatures in pedogenic carbonate laminations on stones at Göbekli Tepe with some other proxy records from the Near East. (a) Main phases of the coating growth rates. (b) $\delta^{13}C$ and $\delta^{18}O$ curves for microlayer successions of pedogenic carbonate; dotted line—L9-80, solid line—L9-66; peak numbers correspond to those in Figure 5d, g; radiocarbon chronology is presented as weighted mean values of calibrated 2ó intervals BP (Table 1); note the difference between the curve forms here and those in Figure 5. (c) Summary of interpretation of the properties of pedogenic carbonate coatings on stones. (d) Holocene time scale in calendar years BP. (e) Slightly simplified representations of some other proxy records from the region: the Mediterranean Sea (deep-sea pollen cores in the eastern part of the sea; Rossignol-Strick, 1999), the Levant (stable isotopic composition of speleothem calcite in the Soreq Cave; Bar-Matthews et al., 1997; Bar-Matthews and Kaufman, 1998), the Dead Sea (fluctuations of the water level; Frumkin and Elitzur, 2002), the Negev Desert (stable isotopic composition of shell calcite in land snails; Goodfriend, 1999), central Anatolia (terrestrial sediment sequences on the Konya Plain; Fontugne et al., 1999 and pollen and geochemical cores from Lake Eski Acigöl; Roberts et al., 2001) and Lake Van (pollen and geochemical cores; Wick et al., 2003).

a water stress (one of the options in (2)). As shown below, this general trend is attributable to an increase in the proportion of C4 flora but the short-term early Holocene $\delta^{13}C$ fluctuations probably need a more complex explanation.

$\delta^{18}O$ values

$\delta^{18}O$ of pedogenic carbonate is determined primarily by the oxygen isotope composition of local meteoric water and may involve evaporative effects (Cerling, 1984; Cerling and Quade, 1993; Amundson et al., 1989, 1996 Quade et al., 1989; Liu et al., 1996). The $\delta^{18}O$ values of secondary carbonate coatings at Göbekli Tepe vary between −11‰ and −7.5‰, with most of them between −9‰ and −8‰ (Fig. 5). There is a general increase in $\delta^{18}O$ values from the oldest to the youngest laminae. The values in curve L9-80 are mostly less negative than in curve L9-66. The latter also displays several distinct negative excursions (peaks 1, 2 and 4), of which the last is especially pronounced and represents an unconformity with the general tendency of increasing $\delta^{18}O$ values in the course of coating growth. In interpreting these data, it is safe to assume that the $^{16}O/^{18}O$ ratio of pedogenic carbonate was negligibly affected if at all by evaporative isotopic phenomena in soil, which are mostly restricted to the uppermost 20–30 cm of a soil profile (Liu et al., 1996; Hsieh et al., 1998).

The generally higher $\delta^{18}O$ values in the youngest pedogenic carbonate laminations suggest a gradual enrichment of the local meteoric water with ^{18}O. For the eastern Mediterranean region, two major factors are supposed to influence an increase in $\delta^{18}O$ of meteoric water: an increase in air temperatures or a decrease in precipitation (Bar-Matthews et al., 1997; Goodfriend, 1999). The contribution of each of these factors is difficult to estimate because most precipitation falls as winter rains and an increase in humidity is expected to produce a similar oxygen isotopic signal as lower air temperatures (Bar-Matthews et al., 1997). Theoretically, changes in original source of moisture in atmospheric precipitation may also lead to shifts in $\delta^{18}O$ values of meteoric water (Amundson et al., 1996; Gat, 1996, and references therein), but this is supposed to have been rather unlikely for the region (Stevens et al., 2001).

If one assumes that atmospheric precipitation was the major factor responsible for the oxygen isotopic composition of pedogenic carbonate at Göbekli Tepe, it would remain unclear why the rates of the coating growth rates were higher in the mid-Holocene than in the early Holocene. Therefore, it seems reasonable to suppose that the oxygen isotopic ratios in atmospheric water and further in pedogenic carbonate were controlled primarily by the air temperatures.

Quantitative temperature estimations for the time of formation of pedogenic carbonate are difficult because of a number of unknown parameters (Cerling and Quade, 1993). However, model relationships between $\delta^{18}O$ of pedogenic carbonate, $\delta^{18}O$ of precipitation and air temperature (Siegenthaler and Matter, 1983; Jiamao et al., 1997) suggest that the coating formation in the mid-Holocene might have proceeded under temperatures up to 5 °C higher than in the early Holocene.

Comparative consideration of the $\delta^{13}C$ and $\delta^{18}O$ records and their paleoecological interpretation

A high correlation between $\delta^{13}C$ and $\delta^{18}O$ in many soils is attributed to the fact that the C4 photosynthetic pathway is favoured by higher temperatures (Cerling and Quade, 1993). This model notion provides a simple explanation for the general increase in both $\delta^{13}C$ and $\delta^{18}O$ values of pedogenic carbonate at Göbekli Tepe from the early Holocene to the mid-Holocene laminae and for the fluctuations in the mid-Holocene $\delta^{13}C$ and $\delta^{18}O$ values (Fig. 8). Given the higher coatings growth rates in the mid-Holocene, these tendencies can be interpreted as warmer and wetter climatic conditions around the mid-Holocene as compared to the early Holocene.

However, this interpretation seems contrary to the isotopic values of the early Holocene pedogenic carbonate microlayers. For sample L9-66, the carbon and oxygen isotopic shifts are the reverse of each other between roughly 10,000 and 6000 cal yr BP, which is especially distinct if one compares peaks 1 and 3 of the $\delta^{13}C$ curve with peaks 1 and 2 of the $\delta^{18}O$ curve, respectively (Fig. 8). A similar tendency is observed in sample L9-80, while much weaker pronounced and only within the first 2–3 kyr of secondary carbonate accumulation: peaks 1 of both $\delta^{18}O$ curves. This regularity is unlikely to originate from changes in the proportion of C4 flora at the site because neither decrease in air temperature nor increase in precipitation (which could theoretically be responsible for more negative $\delta^{18}O$ values) are expected to result in an increase in C4 plant biomass. Presumably some other factors, such as changes in soil respiration rates or/and in the intensity of C3 photosynthetic carbon isotope fractionation (see above), could have determined the carbon isotopic composition of soil CO_2 at Göbekli Tepe in the early Holocene. We suggest that lower temperatures in some periods could have led to reduction in soil respiration, photosynthetic fractionation of carbon isotopes, or both.

In the following we summarize the evidence presented above and propose its paleoenvironmental interpretation (Fig. 8). It should be noted that since in each coating there were only three microlayers with numerical ages, the dating of the periods is based on the assumption of a steady coating growth between the dated microlayers and thus is a provisional model. Further dates will probably lead to a corrected chronology of the secondary carbonate accumulation.

Early Holocene (about 10,000–6000 cal yr BP).   This stage is characterized by a relatively low accumulation rate of pedogenic carbonate on stones and distinct opposite trends in the carbon and oxygen isotopic curves—a decrease in $\delta^{13}C$ and an increase in $\delta^{18}O$ values with several oppositely directed peaks. The peaks are especially pronounced in the oldest part of the microlayer sequence. The most probable paleoecological scenario for the early Holocene is a general increase in air temperatures and a gradual transition towards a more stable climate. We do not see any reason to assume a contribution of CO_2 respired by C4 vegetation, which should have produced a reverse direction of the $\delta^{13}C$ peaks. After a phase of progressive depletion in ^{13}C over the first 1–2 kyr since the beginning of accumulation of pedogenic carbonate, soil CO_2 had reached a

minimum in δ^{13}C values, which may reflect either maximum respiration rates, most intensive photosynthetic carbon fractionation or both. Ecologically, this implies some favourable combination of plant-growth conditions, although it is difficult to differentiate between individual factors. Isotopic signals reflect a persistence of this state of environment with some fluctuations over a period of 2–2.5 kyr. Changes in humidity/aridity during this period are difficult to assess.

Mid-Holocene (about 6000–4000 cal yr BP). The rate of coating growth during most of this period was substantially higher than in the early Holocene, presumably reflecting an increase in humidity. In contrast to the preceding period, the δ^{13}C values of pedogenic carbonate are higher and correlate well with the δ^{18}O values. The carbonate material is generally enriched in ^{18}O in comparison to the first part of the microlayer sequence, suggesting increased air temperatures. At one of the final stages of the formation of coating L9-66, there was also one dramatic negative δ^{18}O excursion (peak 4), originating from a very short cold or humid episode. The fundamental change in the character of relationship between δ^{13}C and δ^{18}O at the transition to the mid-Holocene can be best explained in terms of an advent of C4 component in the local vegetation, presumably stimulated by increased air temperatures. Currently, we have no explanation for the change between the two periods, but one can envision that climatic conditions might have reached a certain temperature threshold near the end of the first period of secondary carbonate formation and became a factor favourable for C4 plants despite increased precipitation.

About 4000 cal yr BP the climate changed irreversibly to more arid conditions. Since the coating growth ceased, no further indications of temperature regime are available for the last 4 kyr.

Comparison with other proxy records in the Near East and the eastern Mediterranean

In general, comparing diverse paleoclimatic records from the region is complicated by several factors: (1) the scarcity of palynological sources, which in turn reflects the low amount of sediments suitable for pollen analysis; (2) insufficient dating of pollen diagrams where they exist and have been studied; and (3) dissimilarity of different proxies (e.g., speleothems and pollen) in their sensitivity to environmental changes. For comparison with the coating record from Göbekli Tepe, we selected some Holocene paleoclimatic records from the Mediterranean Sea, the Levant, central Anatolia and south-eastern Turkey that are well-supplied with numerical dates (Goodfriend, 1999; Rossignol-Strick, 1999; Bar-Matthews et al., 1997; Bar-Matthews and Kaufman, 1998; Frumkin and Elitzur, 2002; Fontugne et al., 1999; Roberts et al., 2001; Wick et al., 2003) (Fig. 8). There are two common features in the character of environmental changes at these sites in the course of the Holocene (Fig. 8). First, all records suggest relatively humid climatic conditions in the early and/or mid-Holocene, in contrast to a relatively arid climate in the late Holocene. Second, the timing of the humid phases ("optima") at different sites probably differed.

As a paleoecological proxy, the secondary carbonate laminations on stones at Göbekli Tepe seem to be in good agreement with the other records from the region. In addition, paleohydrological data by Wilkinson (1999) indicate a change from moderate perennial flows in the early Holocene to stable flows as well as higher water tables in the mid-Holocene at several sites in southern Turkey and northwestern Syria. However, after ca. 4000 cal yr BP there was a decline in the flow stability with a shift to a more erratic flow and accelerated channel aggradation. Of special interest is the geoarchaeological evidence from Kazane Höyük located in close proximity to Göbekli Tepe, suggesting a mid-Holocene environment moister than at present, which gave way to drier conditions at the transition from the Early to Middle Bronze Age, at approximately 4000 cal yr BP (Rosen, 1997). The dry period in the region largely appears to have started with (or even triggered by) the so-called "4.2 ka BP event" (Weiss et al., 1993; Cullen et al., 2000; Courty et al., 2005; Riehl and Bryson, in press).

The record in coatings shows the most resemblance to the lacustrine sediment sequence from Lake Van (Wick et al., 2003) with respect to the Holocene climatic optimum (highest moisture availability) between approximately 6000 and 4000 cal yr BP. The 10- to 8-ka-old layers in this lake are rich in charred plant remains (mostly grass epidermis) bearing witness to steppe fires which, in turn, could be indicative of drought episodes of various intensity or frequency (Wick et al., 2003). Charred plant tissues are characteristic of the oldest 1/5–1/3 of the succession of secondary carbonate microlaminae at Göbekli Tepe. Although the mechanisms of deposition and preservation of charcoal particles in lake sediments and in a soil are different (requiring in the latter case a vertical transport from the soil surface to the Bk horizon), one cannot exclude that their presence in the coatings reflects similar paleoecological events in the region as the charred phytogenic material in Lake Van.

The similarity of the record from Göbekli Tepe to that at Lake Van suggests that much of the northern Fertile Crescent in the early through mid-Holocene might have represented an essentially uniform area in its own right in terms of the geography of environmental patterns, which in turn might have had their consequences for the agricultural origins.

Potential of approach for Quaternary studies in the Near East

The resolution of isotopic record from secondary carbonate microlayers is low when compared, for example, to the well-dated lacustrine sediment sequences cited above. Numerical chronology of each succession of laminae here is restricted by only three ^{14}C dates. Furthermore, radiocarbon dating of pedogenic carbonate still remains a rare practice in Quaternary studies and involves significant uncertainties. However, pedogenic carbonate coatings on stones have a high potential for Quaternary research in two respects. First is their role as paleoecological indicator for regions lacking other proxies. At Göbekli Tepe, two coatings provide a picture of environmental history *in situ* which is consistent with independent paleoclimatic evidence from the region. Moreover, in contrast to pollen cores, pedogenic accumulations of carbonate on stones

represent a proxy record *in situ* and thus can help explain environmental paleopatterns of a territory. Another aspect of the potential use of secondary carbonate laminations is that they can contribute to age determination of soils, sediments and archaeological contexts, in cases where other dating tools cannot be used. Obviously, a careful pedological examination of a context should be preformed prior to sampling and dating procedures in order to minimize possible hazards (e.g., sampling coatings on re-deposited stones). In the Near East, the perspectives of applications of secondary carbonate coatings are especially promising for mountain and hilly landscapes like Upper Mesopotamia, which are rich in stony soils with pedogenic carbonate accumulations.

Conclusions

Pedogenic carbonate coatings on stones at the Pre-Pottery Neolithic site Göbekli Tepe represent a new proxy record for the early-mid Holocene in the northern Fertile Crescent. They formed as a result of pedogenesis and cover the undersides of stones in architectural structures, convex elements of relief representations on megalithic pillars and clasts of the fill. A combination of radiocarbon and the stable carbon and oxygen isotope data from two sequences of coating laminae suggest continuously increasing temperatures at Göbekli Tepe during the early Holocene (ca. 10,000–6000 cal yr BP). In the mid-Holocene (ca. 6000–4000 cal yr BP), the ecology of the site was presumably characterized by its maximum humidity and generally higher temperatures than in the early Holocene. At around 4000 cal yr BP, the climate conditions became relatively dry and never returned to their early to mid-Holocene state in terms of humidity. This model of environmental development in the surroundings of Göbekli Tepe is consistent in its main features with a wide range of environmental proxy records from the eastern Mediterranean and the Near East but appears to give the best fit to the paleoclimatic scenario at Lake Van.

Acknowledgments

References

Alex, M., 1985. Klimadaten ausgewählter Stationen des Vorderen Orients. Beihefte zum Tübinger Atlas des Vorderen Orients. Reihe A (Naturwissenschften) 4, 418.

Ambrose, S.H., Sikes, N.E., 1991. Soil carbon evidence for Holocene habitat change in the Kenya Rift Valley. Science 253, 1402–1405.

Araus, J.L., Febrero, A., Buxo, R., Rodriguez-Ariza, M.O., Molina, F., Camalich, M.D., Martin, D., Voltas, J., 1997. Identification of ancient irrigation practices based on the carbon isotope discrimination of plant seeds: a case study from the south-east Iberian Peninsula. Journal of Archaeological Science 24, 729–740.

Amundson, R., Chadwick, O., Sowers, J., Doner, H., 1989. The stable isotope chemistry of pedogenic carbonates at Kyle Canyon, Nevada. Soil Science Society of America Journal 53, 201–210.

Amundson, R., Wang, Y., Chadwick, O., Trumbore, S., McFadden, L., McDonald, E., Wells, S., DeNiro, M., 1994. Factors and processes governing the ^{14}C content of carbonate in desert soils. Earth and Planetary Science Letters 125, 385–405.

Amundson, R., Chadwick, O., Kendall, C., Wang, Y., DeNiro, M., 1996. Isotopic evidence for shifts in atmospheric circulation patterns during the late Quaternary in mid-North America. Geology 24, 23–26.

Aurenche, O., Galet, P., Régagnon-Caroline, E., Évin, J., 2001. Proto-Neolithic and Neolithic in the cultures in the Middle East—the birth of agriculture, livestock raising, and ceramics: a calibrated ^{14}C chronology 12500–5500 cal BC. Radiocarbon 43 (3), 1191–1202.

Bar-Matthews, M., Kaufman, A., 1998. Middle to Late Holocene (6.500 yr. period) paleoclimate in the eastern Mediterranean region from stable isotopic composition of speleothems from Soreq Cave, Israel. In: Issar, A.S., Brown, N. (Eds.), Water, Environment and Society in Times of Climatic Change. Kluver Academic Publishers, Dordrech, Boston, pp. 203–214.

Bar-Matthews, M., Ayalon, A., Kaufman, A., 1997. Late Quaternary paleoclimate in the eastern Mediterranean region from stable isotope analysis of speleothems at Sorq Cave, Israel. Quaternary Research 47, 155–168.

Birkeland, P., 1999. Soils and Geomorphology. Oxford Univ. Press, New York.

Bottema, S., 1995. The younger Dryas in the Eastern Mediterranean. Quaternary Science Reviews 14, 883–891.

Braidwood, R.J., Howe, B., 1960. Prehistoric investigations in Iraqi Kurdistan. Studies in Ancient Oriental Civilization, 31. University of Chicago Press, Chicago.

Bullock, P., Fedoroff, N., Jongerius, A., Stoops, G., Tursina, T., 1985. Handbook for Soil Thin Section Description. Waine Research, Wolverhampton, UK.

Buck, B.J., Monger, H.C., 1999. Stable isotopes and soil-geomorphology as indicators of Holocene climate change, northern Chihuahuan Desert. Journal of Arid Environments 43, 357–373.

Cerling, T., 1984. The stable isotopic composition of soil carbonate and its relationship to climate. Earth and Planetary Science Letters 71, 229–240.

Cerling, T., 1991. Carbon dioxide in the atmosphere: evidence from cenozoic and mesozoic paleosols. American Journal of Science 291, 377–400.

Cerling, T., Quade, J., 1993. Stable carbon and oxygen isotopes in soil carbonates. Climate change in continental isotopic records. Geophysical Monograph 78, 217–231.

Cerling, T., Quade, J., Wang, Y., Bowman, J.R., 1989. Carbon isotopes in soils and paleosoils as ecology and paleoecology indicators. Nature 341, 138–139.

Childe, V.G., 1952. New Light on the Most Ancient East. Praeger, New York.

Courty, M.-A., Goldberg, P., McPhail, R.I., 1989. Soils and micromorphology in archaeology. Cambridge Manuals in Archaeology. Cambridge Univ. Press, Cambridge.

Courty, M.-A., Marlin, C., Dever, L., Tremblay, P., Vachier, P., 1994. The properties, genesis and environmental significance of calcitic pendents from the high arctic (Spitsbergen). Geoderma 61, 71–102.

Courty, M.-A., Crisci, A., Fedoroff, N., Greenwood, P., Grice, K., Leroy, E., Mermoux, M., Pastol, J.L., Smith, D., Thiemens, M., 2005. Consequences on humans, lands and climate of the 4-kyr BP impact across the Near East. The General Assembly of European Geosciences Union, Vienna, 24–29 April 2005. Abstract EGU05-A-04746.

Cullen, H.M., deMenocal, P.B., Hemming, S., Hemming, G., Brown, F.H., Guilderson, T., Sirocko, F., 2000. Climate change and the collapse of the Akkadian empire: evidence from the dead sea. Geology 28 (4), 379–382.

Deutz, P., Montanez, I.P., Monger, H.C., Morrison, J., 2001. Morphology and isotope heterogeneity of Late Quaternary pedogenic carbonates: implications for paleosol carbonates as paleoenvironmental proxies. Palaeogeography, Palaeoclimatology, Palaeoecology 166, 293–317.

Ferrio, J.P., Florit, A., Vega, A., Serrano, L., Voltas, J., 2003. Δ^{13}C and tree-ring width reflect different drought responses in *Quercus ilex* and *Pinus halepensis*. Oecologia 442, 512–518.

Fontugne, M., Kuzucuoðlu, C., Hatté, C., Pastre, J.-F., 1999. From Pleniglacial to Holocene: in the Konya Plain, Turkey. Quaternary Science Reviews 18, 573–591.

Frumkin, A., Elitzur, Y., 2002. Historic Dead Sea level fluctuations calibrated with geological and archaeological evidence. Quaternary Research 57, 334–342.

Frumkin, A., Ford, D.C., Schwarcz, H., 1999. Continental oxygen isotopic record of the last 170.000 years in Jerusalem. Quaternary Research 51, 317–327.

Gat, J.R., 1996. Oxygen and hydrogen isotopes in the hydrological cycle. Annual Review of Earth and Planetary Sciences 24, 225–262.

Goldberg, P., 1994. Interpreting Late Quaternary continental sequences in Israel. In: Bar-Yosef, O., Kra, R.S. (Eds.), Late Quaternary Chronology and Paleoclimates of the Eastern Mediterranean. Tucson, Radiocarbon, pp. 89–102.

Goodfriend, G.A., 1999. Terrestrial stable isotope record of Late Quaternary paleoclimates in the eastern Mediterranean region. Quaternary Science Reviews 18, 501–513.

Guidelines for Soil Profile Description, 1990. Third edition (revised). Soil Resources, Management, and Conservation Service, Land and Water Development Division. Rome: FAO.

Heun, M., Schäfer-Bregl, R., Klawan, D., Castagna, R., Accerbi, M., Borghi, B., Salamini, F., 1997. Site of einkorn domestication identified by DNA fingerprinting. Science 278, 1312–1314.

Hsieh, J.C.C., Chadwick, O.A., Kelly, E.F., Savin, S.M., 1998. Oxygen isotopic composition of soil water: quatifying evaporation and transpiration. Geoderma 82, 269–293.

Jiamao, H., Keppens, E., Tungsheng, L., Paepe, R., Wenying, J., 1997. Stable isotope composition of the carbonate concretions in loess and climate change. Quaternary International 37, 37–43.

Khokhlova, O.S., Khokhlov, A.A., Chichagova, O.A., Morgunova, N.L., 2004. Radiocarbon dating of calcareous accumulations in soils of the Holocene chronosequence in the Ural river valley (Cis-Ural steppe). Eurasian Soil Science 37 (10), 1024–1038.

Körner, C., Farquhar, G.D., Wong, S.C., 1991. Carbon isotope discrimination by plants follows latitudinal and altitudinal trends. Oecologia 88, 30–40.

Kurapkat, D. 2004. Die frühneolithischen Bauanlagen auf dem Göbekli Tepe in Obermesopotamien (Südosttürkey). Bericht über die 42. Tagung für Ausgrabungswissenschaft und Bauforschung 2002 in München. Koldewey-Gesellschaft. Stuttgart. 256–267.

Liu, B., Philips, F.P., Campbell, A.R., 1996. Stable carbon and oxygen isotopes of pedogenic carbonates, Ajo Mountains, southern Arizona: implications for paleoenvironmental change. Palaeogeography, Palaeoclimatology, Palaeoecology 124, 233–246.

Monger, H.C., Cole, D.R., Gish, J.W., Giordano, T.H., 1998. Stable carbon and oxygen isotopes in Quaternary soil carbonates as indicators of ecogeomorphic changes in the northern Chihuahuan Desert, USA. Geoderma 82, 137–172.

Mora, G., Pratt, L., 2002. Carbon isotopic evidence from paleosols for mixed C3/C4 vegetation in the Bogota Basin, Colombia. Quaternary Science Reviews 21, 985–995.

Neef, R., 2003. Overlooking the steppe-forest: a preliminary report on the botanical remains from Early Neolithic Göbekli Tepe (Southeastern Turkey). Neo-Lithics 2/03, 13–16.

Nesbitt, M., 2002. When and where did domesticated cereals first occur in southwest Asia. In: Cappers, R.T.J., Bottema, S. (Eds.), The Dawn of Farming in the Near East. Ex Oriente, Berlin, pp. 113–132.

Nordt, L., Wilding, L., Hallmark, C., und Jacob, J., 1996. Stable carbon isotope composition of pedogenic carbonates and their use in studying pedogenesis. In: Boutton, T.W., Yamasaki, S. (Eds.), Mass spectrometry of soils. Marcel Dekker, Inc., New York, pp. 133–154.

Pamir, H.N., Erentöz, C., 1974. Geological Map of Turkey, 1:500000. Diyarbakir Sheet. MTA. Ankara.

Pendall, E., Harden, J., Trumbore, S., Chadwick, O., 1994. Isotopic approach to soil carbonate dynamics and implications for paleoclimatic interpretations. Quaternary Research 42, 60–71.

Peters, J., Schmidt, K., 2004. Animals in the symbolic world of Pre-Pottery Neolithic Göbekli Tepe, south-eastern Turkey: a preliminary assessment. Anthropozoologica 39 (1), 179–218.

Pustovoytov, K., 2002. Pedogenic carbonate cutans on clasts in soils as a record of history of grassland ecosystems. Palaeogeography, Palaeoclimatology, Palaeoecology 177, 199–214.

Pustovoytov, K., 2006. Soils and soil sediments at Göbekli Tepe: a preliminary report. Geoarchaeology 21 (7), 699–719.

Pustovoytov, K., Leisten, T., 2002. Diagenetic alteration of artificial lime mortar in a Mediterranean soil: ^{14}C and stable carbon isotopic data. 17th World Congress of Soil Science, 14–21 August, Bangkok.

Quade, J., Cerling, T., Bowman, R., 1989. Systematic variations in the carbo and oxygen isotopic composition of pedogenic carbonate along elevation transects in the southern Great Basin, United States. Geological Society of America Bulletin 101, 464–475.

Ramsey, B.C., 2001. Development of the Radiocarbon Program OxCal. Radiocarbon 43 (2A), 355–363.

Riehl, S., Bryson, R., in press. Variability in human adaptation to changing environmental conditions in Upper Mesopotamia during the Early and the Middle Bronze Age. Varia Anatolica.

Roberts, N., Black, S., Boyer, P., Eastwood, W.J., Griffiths, H.I., Lamb, H.F., Leng, M.J., Parsih, R., Reed, J.M., Twigg, D., Yiitbasioglu, H., 1999. Chronology and stratigraphy of Late Quaternary sediments in the Konya Basin, Turkey: results from the KOPAL Project. Quaternary Science Reviews 18, 611–630.

Roberts, N., Reed, J.M., Leng, M.J., Kuzucuoglu, C., Fonutgne, M., Bertaux, J., Woldring, H., Bottema, S., Black, S., Hunt, E., Karabiyikoglu, M., 2001. The tempo of Holocene climatic change in the Eastern Mediterranean region: new high-resolution crater-lake sediment data from central Turkey. The Holocene 11 (6), 721–736.

Robinson, S.A., Black, S., Sellwood, B.W., Valdes, P.J., 2006. A review of palaeoclimates and palaeoenvironments in the Levant and Eastern Mediterranean from 25,000 to 5000 years BP: setting the environmental background for the evolution of human civilisation. Quaternary Science Reviews 25, 1517–1541.

Rosen, A.M., 1997. The geoarchaeology of Holocene environments and land use at Kazane Höyük, SE Turkey. Geoarchaeology 12 (4), 395–416.

Rossignol-Strick, M., 1999. The Holocene climatic optimum and pollen records of sapropel 1 in the eastern Mediterranean, 9000–6000 BP. Quaternary Science Reviews 18, 515–530.

Sage, R.F., 2001. Environmental and evolutionary preconditions for the origin and diversification of the C4 photosynthetic syndrome. Plant Biology 3, 202–213.

Schleser, G.H., Jajasekera, R., 1985. δ^{13}C-variations of leaves in forests as an indication of reassimilated CO$_2$ from the soil. Oecologia 65, 536–542.

Schmidt, K., 2001. Göbekli Tepe, Southeastern Turkey. A preliminary report on the 1995–1999 excavations. Paléorient 26/1, 45–54.

Schmidt, K., 2002. The 2002 excavations at Göbekli Tepe (Southeastern Turkey)—impressions from an enigmatic site. Neo-Lithics 2/02, 8–13.

Schmidt, K., 2003. The 2003 campaign at Göbekli Tepe (Southeastern Turkey). Neo-Lithics 2/03, 3–8.

Siegenthaler, U., Matter, H.A., 1983. Dependence of δ^{18}O and δD in precipitation on climate. Palaeoclimate and palaeowaters. A Collection of Environmental Isotope Studies. IAEA, pp. 37–51.

Snyder, J.A., Wasylik, K., Fritz, S., Wright Jr., H.E., 2001. Diatom-based conductivity reconstruction and paleoclimatic interpretation of a 40-ka record from Lake Zeribar, Iran. The Holocene 11 (6), 737–745.

Spötl, C., Vennemann, T., 2003. Continuous-flow isotope ratio mass spectrometric analysis of carbonate minerals. Rapid Communications in Mass Spectrometry 17, 1004–1006.

Stevens, J.A., Wright Jr., H.E., Ito, E., 2001. Proposed changes in seasonality of climate during the Late-glacial and Holocene at Lake Zeribar, Iran. The Holocene 11 (6), 745–755.

Straub, R., 1988. Bodengesellschaften des Vorderen Orients. Beihefte zum Tübinger Atlas des Vorderen Orients. Reihe A (Naturwissenschaften), Nr. 16. Wiesbaden: Dr. Ludwig Reichert.

Tieszen, L.L., 1991. Natural variations in the carbon isotope values of plants: implications for archaeology, ecology and paleoecology. Journal of Archaeological Science 18, 227–248.

Van Zeist, W., Bottema, S., 1991. Late Quaternary vegetation of the Near East. Beihefte zum Tübinger Atlas des Vorderen Orients. Reihe A (Naturwissenschaften). Nr. 18. Dr. Ludwig Reichert Verlag. Wiesbaden. 156 pp.

Wang, Y., Amundson, R., Trumbore, S., 1994. A model of $^{14}CO_2$ and its implications for using ^{14}C to date pedogenic carbonate. Geochemistry Cosmochemistry Acta 58, 393–399.

Wang, Y., McDonald, E., Amundson, R., McFadden, L., Chadwick, O., 1996. An isotopic study of soils in chronological sequences of alluvial deposits, Providence Mountains, California. Geological Society of America Bulletin 108, 379–391.

Warren, C.R., McGrath, J.F., Adams, M.A., 2001. Water availability and carbon isotope discrimination in conifers. Oecologia 127, 476–486.

Weiss, H., Courty, M.-A., Wetterstrom, W., Guichard, F., Senior, L., Meadow, R.A., Curnow, A., 1993. The genesis and collapse of the third millennium north Mesopotamian civilization. Science 261, 995–1004.

Wick, L., Lemcke, G., Sturm, M., 2003. Evidence of Lateglacial and Holocene climatic change and human impact in eastern Anatolia: high-resolution pollen, charcoal, isotopic and geochemical records from the laminated sediments of Lake Van, Turkey. Holocene 13 (5), 665–675.

Wilkinson, T.J., 1999. Holocene valley fills of southern Turkey and NW Syria: recent geoarchaeological contributions. Quaternary Science Reviews 18, 555–572.

Williams, D.G., Ehleringer, J.R., 1996. Carbon isotope discrimination in three semi-arid woodland species along a monsoon gradient. Oecologia 106, 455–460.

World Reference Base for Soil Resources, 1998. FAO Report Nr 84. Rome: FAO.

Yasuda, Y., Kitagawa, H., Nakagawa, T., 2000. The earliest record of major anthropogenic deforestation in the Ghab Valley, northwest Syria: a palynological study. Quaternary International 73/74, 127–136.

Zohary, D., Hopf, M., 2000. Domestication of plants in the Old World: the origin and spread of cultivated plants in West Asia, Europe and the Nile Valley, third ed. Oxford University Press. Oxford, UK, p. 278.